

Shot noise in transport through “double quantum dots”

Jasmin Aghassi,^{1,2,3} Axel Thielmann,^{1,2,3} Matthias H. Hettler,¹ and Gerd Schön^{1,2,3}

¹*Forschungszentrum Karlsruhe, Institut für Nanotechnologie, 76021 Karlsruhe, Germany*

²*Institut für Theoretische Festkörperphysik, Universität Karlsruhe, 76128 Karlsruhe, Germany*

³*Center for Functional Nanostructures (CFN), Universität Karlsruhe, 76128 Karlsruhe, Germany*

(Dated: February 5, 2008)

Motivated by activities of several experimental groups we investigate electron transport through two coherent, strongly coupled quantum dots (“double quantum dots”), taking into account both intra- and inter-dot Coulomb interactions. The shot noise in this system is very sensitive to the internal electronic level structure of the coupled dot system and its specific coupling to the electrodes. Accordingly a comparison between experiments and our predictions should allow for a characterization of the relevant parameters. We discuss in detail the effect of asymmetries, either asymmetries in the couplings to the electrodes or a detuning of the quantum dot levels out of resonance with each other. In the Coulomb blockade region super-Poissonian noise appears even for symmetric systems. For bias voltages above the sequential tunneling threshold super-Poissonian noise and regions of negative differential conductance develop if the symmetry is broken sufficiently strongly.

PACS numbers: 73.63.-b, 73.23.Hk, 72.70.+m

I. INTRODUCTION

While early studies of electron transport through mesoscopic systems such as quantum dots or molecular systems concentrated on the current^{1,2}, more recent activities, both experimental^{3,4,5,6} and theoretical^{7,8,9,10,11,12,13,14,15,16,17,18}, include the analysis of shot noise. The latter provides additional insight into the quantum transport properties¹⁹ and allows a more detailed characterization of the quantum transport device.

For ‘local’ systems, such as single (multilevel) quantum dots, above the sequential tunneling threshold the shot noise power S is typically sub-Poissonian, implying that the Fano factor $F = S/2eI$, where I is the mean current, is less than unity. If the level couplings are asymmetric, e.g. in the presence of magnetically polarized electrodes, the noise can become super-Poissonian. In this case the Fano factor takes values larger than unity^{7,13}. Very recently it was found that enhanced noise can also be found in symmetric systems inside the Coulomb blockade region where the current is much suppressed^{10,14,20}. On the other hand, for ‘non-local’ systems, such as serially coupled quantum dots, due to their complex internal level structure, super-Poissonian noise can develop even in fully symmetric situations and above the sequential tunneling threshold¹⁸. These ‘non-local’ systems exhibit a pronounced and sensitive dependence of their transport characteristics on internal parameters and couplings.

In this article we study sequential transport in a system of two strongly coupled quantum dots. Specifically, we consider a double quantum dot (DQD) in series in which the left dot is coupled weakly to left electrode and similarly the right dot to the right electrode, while the two dots are coupled strongly via electron tunneling, and they also interact electrostatically via the Coulomb interaction (see Section II). Our results (in Section III) address two distinct issues:

(i) In Section III A we study the shot noise of the

symmetrically coupled DQD in the Coulomb blockade regime, generalizing the work of Ref. 20. Co-tunneling processes are assumed to be weak, hence transport is due only to thermally activated processes. We find that in the Coulomb blockade regime the relation between two energy scales, the sequential tunneling energy ϵ_{seq} and the difference of the first excitation energy and the ground state (which is also the inelastic cotunneling energy) ϵ_{co} , determines the occurrence or absence of super-Poissonian noise. This part of our analysis is valid generally for weakly coupled system in the Coulomb blockade regime, for any value of the gate voltage, as it depends only on generic properties of the internal electronic structure of the interacting dot system.

(ii) Above the sequential tunneling threshold, for the weakly coupled DQD super-Poissonian noise can only appear if the left \leftrightarrow right symmetry is broken. For a non-local system like the DQD this symmetry breaking can be achieved in two qualitative different ways: (a) The symmetry of the electrode-dot couplings is broken, while the DQD is unchanged, see Section III B. Here, the step positions in the current and noise characteristics are not influenced by the asymmetry. But for sufficient asymmetry in the coupling negative differential conductance (NDC) appears, i.e. the current decreases with increasing bias, while at even stronger asymmetry additionally super-Poissonian noise appears. (b) The symmetry of the electrode-dot couplings is preserved, while the symmetry of the DQD-Hamiltonian is broken by detuning the dot level energies, see Section III C. Here, the step positions in the current and noise characteristics differ for different degrees of detuning. The DQD eigenfunctions become spatially non-uniform which breaks the parity symmetry of the effective coupling of the various eigenstates to the electrodes. This, in turn, leads again to NDC and eventually with further detuning to super-Poissonian noise.

As such asymmetries are easily detected in an experiment, we can learn more about the underlying asymme-

tries of the couplings, electronic structure and also the total spin of the states participating in transport. In the available measurements setups on DQDs of various groups^{21,22,23,24} metallic finger gates allow for controlled manipulation of the relevant parameters, e.g the electrostatic potential of the individual dots as well as the inter-dot and dot-electrode couplings. While it might be difficult to unambiguously distinguish the two cases of symmetry breaking, our predictions should still be verifiable in shot noise measurements in available systems. We also comment and compare our results to related theoretical work^{8,11,12} on similar systems in Section III D. We conclude with a summary in Section IV.

II. MODEL AND TECHNIQUE

We consider two coupled quantum dots, each with a sufficiently large level spacing such that we can restrict ourselves to one spin-degenerate level per dot. Including electron hopping between the dots as well as intra-dot and inter-dot (nearest neighbor) Coulomb interactions we arrive at the Hamiltonian $\hat{H} = \hat{H}_L + \hat{H}_R + \hat{H}_{\text{DQD}} + \hat{H}_{\text{T,L}} + \hat{H}_{\text{T,R}}$ with

$$\begin{aligned} \hat{H}_r &= \sum_{k\sigma} \epsilon_{k\sigma r} a_{k\sigma r}^\dagger a_{k\sigma r}, \quad \hat{H}_{\text{T},r} = \sum_{ik\sigma} (t_r a_{k\sigma r}^\dagger c_{i\sigma} + h.c.), \\ \hat{H}_{\text{DQD}} &= \sum_{i\sigma} \epsilon_i n_{i\sigma} - t \sum_{\sigma} (c_{1\sigma}^\dagger c_{2\sigma} + h.c.) \\ &+ U \sum_i n_{i\uparrow} n_{i\downarrow} + U_{nn} \sum_{\sigma\sigma'} n_{1\sigma} n_{2\sigma'}, \end{aligned} \quad (1)$$

where $i = 1, 2$ denote the dot levels and $r = \text{L, R}$. Here, \hat{H}_L and \hat{H}_R model the non-interacting electrons with density of states $\rho_e = \sum_k \delta(\omega - \epsilon_{k\sigma r})$ in the left and right electrode ($a_{k\sigma r}^\dagger, a_{k\sigma r}$ are the Fermi operators for the states in the electrodes). The chemical potentials (Fermi energy) of the electrodes μ_L, μ_R in equilibrium set the zero point of the energy scale. The term \hat{H}_{DQD} describes the coupled dots with on-site energy ϵ_i and inter-dot hopping t . $c_{i\sigma}^\dagger, c_{i\sigma}$ are Fermi operators for the molecular levels, and $n_{i\sigma} = c_{i\sigma}^\dagger c_{i\sigma}$ is the number operator. The strength of the intra-dot and inter-dot Coulomb repulsion is given by U and U_{nn} respectively. The parameters U and U_{nn} can be related to the charging energies of the dots and the various capacitances when comparing to experimental setups as described e.g. in Ref. 2. Other electron interaction terms could be considered by much more elaborate models, as done in Ref. 26 for computation of the $I - V$ characteristics. For the effects on the shot noise that we wish to study, the simpler model above suffices. The terms $\hat{H}_{\text{T,L}}$ and $\hat{H}_{\text{T,R}}$ describes tunneling between the leads and the corresponding adjacent dot. The respective coupling strength is characterized by the intrinsic line width $\Gamma_r = 2\pi |t_r|^2 \rho_e$, where t_r are the tunneling matrix elements.

We are interested in transport through the DQD, in particular in the current I and the (zero-frequency) current noise S . They are related to the current operator $\hat{I} = (\hat{I}_R - \hat{I}_L)/2$, with $\hat{I}_r = -i(e/\hbar) \sum_{ik\sigma} (t_i^r a_{k\sigma r}^\dagger c_{i\sigma} - h.c.)$ being the current operator for electrons tunneling into lead r , by $I = \langle \hat{I} \rangle$ and

$$S = \int_{-\infty}^{\infty} dt \langle \delta \hat{I}(t) \delta \hat{I}(0) + \delta \hat{I}(0) \delta \hat{I}(t) \rangle \quad (2)$$

where $\delta \hat{I}(t) = \hat{I}(t) - \langle \hat{I} \rangle$.

We compute transport via a master equation for the diagonal elements of the reduced density matrix of the DQD system. This approach has been discussed in detail in Ref. 13. For completeness, here we summarize the most salient aspects of this approach. The reduced density matrix is expressed in the eigenstate basis of the dot Hamiltonian H_{DQD} , Eq.1. For the $N = 2$ dot system there exist $4^N = 16$ eigenstates χ of the form $\chi = \sum_s c_s |s\rangle$, where $|s\rangle$ denotes a basis state of the form $|n_{1\uparrow} n_{1\downarrow} n_{2\uparrow} n_{2\downarrow}\rangle$ and the c_s are the corresponding coefficients. The analytic form of the eigenstates and eigenvalues of our Hamiltonian can be found in Ref. 27. We calculate the transition rates \mathbf{W} between the eigenstates via perturbation theory (in this case via the Fermi golden rule) in the electrode-DQD couplings Γ^r . The bold face indicates matrix notation related to the eigenstate labels χ . In the stationary situation (no explicit time dependence of the bias) the density matrix becomes time independent and we can find the average occupation of the eigenstates, i.e. stationary probabilities \mathbf{p}^{st} by the solution of the master rate equation

$$\sum_{\chi'} W_{\chi, \chi'} p_{\chi'}^{\text{st}} = 0. \quad (3)$$

under the condition that $\sum_{\chi} p_{\chi}^{\text{st}} = 1$. For the calculation of the current I and current noise S , we use the diagrammatic technique on the Keldysh contour developed in Ref. 28 which was expanded for the description of the noise in Ref. 13. In first order perturbation theory, the current and shot noise are given by:

$$I = \frac{e}{2\hbar} \mathbf{e}^T \mathbf{W}^I \mathbf{p}^{\text{st}} \quad (4)$$

$$S = \frac{e^2}{\hbar} \mathbf{e}^T (\mathbf{W}^{II} \mathbf{p}^{\text{st}} + \mathbf{W}^I \mathbf{P} \mathbf{W}^I \mathbf{p}^{\text{st}}). \quad (5)$$

The vector \mathbf{e} is given by $e_{\chi} = 1$ for all χ . The objects $\mathbf{W}^I (\mathbf{W}^{II})$ denote the Laplace transform of the transition rates (in the time domain) between eigenstates χ with one (two) current vertex(ices) due to \hat{I}_r , replacing a tunneling vertex due to $H_{\text{T,L}}$ or $H_{\text{T,R}}$. The "propagator" \mathbf{P} can be found from the Dyson equation. In first order perturbation theory it is obtained from the equation

$$\mathbf{P} = \tilde{\mathbf{W}}^{-1} \mathbf{Q}, \quad (6)$$

where $\tilde{\mathbf{W}}$ is identical to the transition rates matrix \mathbf{W} defined above but with one row (arbitrarily chosen) χ_0 being replaced with (Γ, \dots, Γ) and $Q_{\chi\chi'} = (p_{\chi'}^{st} - \delta_{\chi'\chi})(1 - \delta_{\chi'\chi_0})$, see Ref. 13 for the full details.

We point out that expression Eq. 5 consists of two terms. The first term, denoted by S_{irr} is due to \mathbf{W}^{II} , i.e. the noise diagrams with two current vertices in a single irreducible block. The second term, denoted by S_{red} , is due to reducible noise diagrams, i.e. diagrams with a "propagator" \mathbf{P} between the two current vertices of Eq. 2 at different times. It therefore accounts for the electronic structure and the correlations of the system. It is mostly the second term S_{red} that is responsible for the interesting correlation physics and super-Poissonian noise, as we will see below.

III. RESULTS

In the following we discuss current and shot noise for systems described by a Hamiltonian of the type of Eq. (1) in first order perturbation theory in the tunnel couplings Γ_r . In the first part of the discussion special emphasis is put on examining the behavior of the Fano factor (Noise) in the Coulomb blockade region. The second part will be devoted to the discussion of asymmetry effects induced to the double dot system by asymmetric coupling to the leads or detuned level energies, respectively. In the case of symmetric couplings we choose $\Gamma_L = \Gamma_R = 2.5\mu\text{eV}$ defining a total line width of $\Gamma = \Gamma_L + \Gamma_R = 5\mu\text{eV}$. (We choose this explicit energy scale as we are varying a number of different energy parameters in the following.) Our perturbation expansion is valid for temperatures much larger than the tunnel couplings. Throughout this paper, we choose $k_B T = 10\Gamma$ which translates to $T = 50\mu\text{eV} \sim 0.6\text{K}$. The dot system is characterized by the level energies ϵ_i , the intra-dot 'Hubbard' repulsion U , and the nearest neighbor charge repulsion U_{nn} . If not stated otherwise the level energies are chosen to be resonant, $\epsilon_1 = \epsilon_2 = \epsilon$.

A current is driven by an applied bias voltage $V_b = \mu_L - \mu_R$. We assume the voltages to drop symmetrically and, since the dot-electrode coupling is weak compared to the dot-dot coupling, entirely at the electrode-dot tunnel junctions. This implies that the level energies of the dots are independent of the applied voltage. Effects such as level detuning due to asymmetric or incomplete voltage drops and or applied gate voltages could easily be included. We do not consider these effects here, as they add unnecessary complexity to the results presented below. We include only a single level per dot (plus interactions), assuming that the level spacing within each dot is larger than all other energy scales.

To proceed we diagonalize the dot Hamiltonian H_{DQD} including the interaction terms. The resulting eigenstates can be organized according to the two quantum numbers: total charge $-qe$ (with q an integer, $q \in 0, 1, 2, 3, 4$) and total spin (singlets, doublets and triplets for our DQD

model)^{27,31}. As the onsite energies ϵ_i are decreased to lower, negative values (experimentally achieved by a gate voltage applied to both dots) the ground state charge shifts from $q = 0$ to increasing values $q = 1, q = 2 \dots$. While previous work^{8,11} has focused mostly on the zero charge ($q = 0$) ground state we study the more interesting case (see below) with a "half filled" ground state ($q = 2$), where the low-bias transport sensitively depends on the spatial and spin structure of the eigenstates in the various charge sectors.

For the sequential transport in quantum dot systems at low bias two energy scales are relevant: (1) The "sequential energy gap" ϵ_{seq} denotes the energy difference between the ground state with charge $-qe$ and the first excited states with the charge $-(q+1)e$ ('anion ground state') or with charge $-(q-1)e$ ('cation ground state'), depending on which one is smaller. The sequential tunneling threshold, i.e. the bias above which the current is no longer suppressed due to Coulomb blockade, is reached at $V = 2\epsilon_{seq}/e$ for symmetric bias. (2) The energy gap between the ground state with charge $-qe$ and the first excited state with the same charge, denoted in the following by ϵ_{co} . The energy ϵ_{co} is also known as the 'vertical' gap, and is related to the HOMO-LUMO gap in molecular systems. It would be the energy scale relevant for inelastic co-tunneling processes. Note, however, that co-tunneling processes, which are of second order in Γ_r , are not included in this work. If one would start with a ground state of zero charge ($q = 0$) the energy scale ϵ_{co} would not exist within our model, due to the restriction to single level dots. As we consider the case of a half filled ground state we avoid such an artefact. Also note that recent experiments on double quantum dot systems with applications for quantum computing^{23,24,25} work with ground states of non-zero charge.

A. Symmetrically coupled quantum dots

We begin with a system of two dots in series and energy parameters such that the DQD is half filled in the ground state (no bias applied). In the right panel of Fig.1 part of the energy excitation spectrum resulting from the diagonalization of the Hamiltonian is displayed. The ground state G is a singlet state (total spin 0) and charge $-2e$ ($q = 2$). It is delocalized over the two dots (a combination of the four two electron singlet basis vectors $|s\rangle$) with an eigenvalue E_G dependent on all parameters of H_{DQD} , $E_G = 2\epsilon + 1/2(U + U_{nn} - \Delta)$, where²⁷ $\Delta = \sqrt{16t^2 + (U - U_{nn})^2}$. The first excited state is the bonding state B with $q = 1$. It is a doublet with total spin 1/2, eigenvalue $\epsilon - t$, and is also delocalized over both dots. Therefore, the energy scale ϵ_{seq} is given $\epsilon_{seq} = E_B - E_G$. The second excited state is a triplet (total spin 1) with $q = 2$. In the triplet state one electron each is "fixed" to one dot. Therefore, its eigenvalue is independent of the inter-dot hopping t and the on-site repulsion U . the energy scale ϵ_{co} is therefore given by

$\epsilon_{co} = E_T - E_G$. The rest of the spectrum is not shown, since for the following discussion we will refer to a bias regime for which other states are not yet important. The higher excited states are responsible for the step features above $V_b \sim 5mV$. Note that in the artificial limit $U \rightarrow \infty$ the energy scale ϵ_{co} vanishes. In this case, the triplet and singlet states would be degenerate and some of the effects described below would disappear.

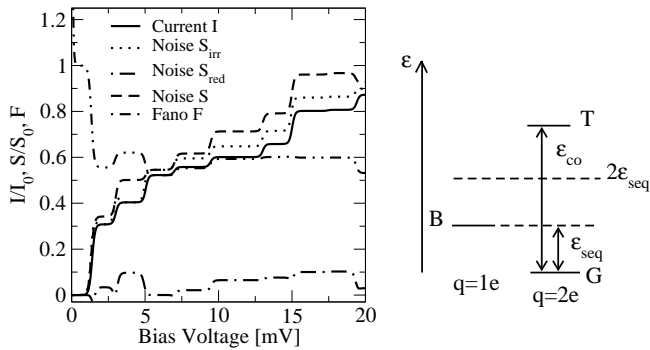


FIG. 1: *Left panel:* Current I and shot noise S vs. bias voltage for a double dot system with $k_B T = 0.05$, $t = 2$, $U = 10$, $U_{nn} = 5$ and $\epsilon = -5.5$ resulting in a doubly occupied ground state ($q = 2e$), all units in meV. The noise S is sub-Poissonian for all bias voltages. This is always the case if the first vertical excitation energy is larger than twice the sequential tunneling threshold, $\epsilon_{co} > 2\epsilon_{seq}$, see the sketch in the right panel. Current and noise curves are normalized to $I_0 = (e/h)2\Gamma$ and $S_0 = (e^2/h)2\Gamma$, respectively. *Right panel:* sketch of the low energy spectrum. The nature of the states G, T and B is discussed in the text.

Fig.1 shows the typical behavior for a fully symmetric system with $\epsilon_{co} > 2\epsilon_{seq}$: both current and noise rise monotonically in steps, while the Fano factor will fall between values of 1 (Poissonian noise) and 1/2 (symmetric double barrier noise) for the large bias region, i.e. a bias voltage larger than all excitation energies. In general, the Fano factor will not fall with a monotonous dependence on the bias. This non-monotonicity is due to the second term in the noise expression Eq. 5, associated with the propagator \mathbf{P} , which can give positive and negative contributions (it is negative in the entire Coulomb blockade region and becomes positive only on the first plateau). In the Coulomb blockade current and noise are both (equally) exponentially suppressed resulting in a Fano factor of Poissonian value. At small bias, $eV_b \ll k_B T$, the noise is dominated by thermal noise, described by the well known hyperbolic cotangent behavior which leads to a divergence of the Fano factor^{19,32}.

If we now lower the onsite energy ϵ we energetically favor states with larger charge and thus increase the energy ϵ_{seq} as compared to the situation as shown in the right panel of Fig.1, while preserving the energy ϵ_{co} . Thereby, we can realize a situation in which $\epsilon_{seq} < \epsilon_{co} < 2\epsilon_{seq}$, see Fig.2. Above the sequential threshold the current and noise curve look very similar to the situation in Fig. 1, with the expected small shifts in the step positions.

However, in the Coulomb blockade region the Fano factor behaves differently to before. After the region of thermal noise accompanied with divergent Fano factor, a Poissonian value of $F = 1$ is reached. For higher bias and close to (but still below) the sequential tunneling threshold a peak like feature (actually a short plateau) appears in the Fano factor. This is caused by a relative enhancement of the noise, visible in Figs. 2 and 4 by the apparent shift of the noise curve to lower bias in the left panel. The increase of the Fano factor is due to the second term in the noise expression S_{red} (Eq. 5), see the Fig.3 (note the semi-logarithmic scale). The first part of the noise S_{irr} provides the finite thermal noise around zero bias. It then grows with bias with the same exponential behavior as the current and contributes a Poissonian term $2eI$ to the shot noise. In contrast, the (now positive) second part S_{red} becomes only appreciable for a bias $V_b > (\epsilon_{co} - \epsilon_{seq})/e$ and renders the shot noise super-Poissonian above this bias. This noise enhancement is due to the possible thermal occupation and subsequent sequential depletion of excited states that lead to small cascades of tunneling events interrupted by long (Coulomb) blockages. The alternation of these processes with different time scales results in a noisy current. Consequently, the Fano factor is larger than unity, indicating super-Poissonian noise. This effect was recently discussed in some detail by Belzig and co-workers^{10,20}, for systems restricted to a singly occupied ground state. At a bias higher than the sequential threshold the noise recovers sub-Poissonian behavior.

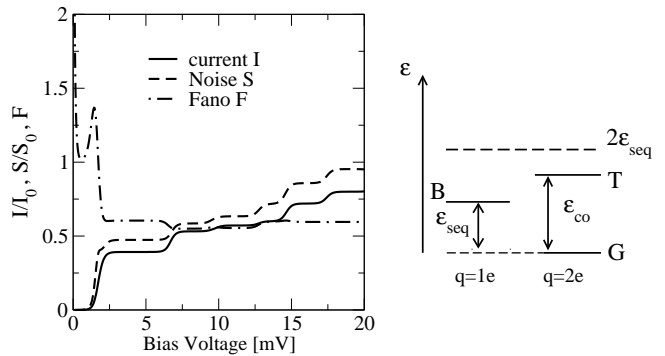


FIG. 2: *Left panel:* Current I and shot noise S vs. voltage for a double dot system with $k_B T = 0.05$, $t = 2$, $U = 12$, $U_{nn} = 4meV$ and $\epsilon = -5.3$. Super-Poissonian noise (Fano factor $F > 1$) develops in the Coulomb blockade regime. *Right panel:* low energy spectrum, where now $\epsilon_{seq} < \epsilon_{co} < 2\epsilon_{seq}$.

For the same parameters as above but with further lowered onsite energy $\epsilon = -6.3$ we obtain a situation where $\epsilon_{co} < \epsilon_{seq}$. The current, noise and Fano factor for such a situation are depicted in Fig. 4. For a bias larger than the sequential tunneling threshold the curves show again generic behavior as displayed in Fig. 1 and Fig.2. However, in the Coulomb blockade regime and after divergent thermal noise behavior we directly obtain a super-Poissonian Fano factor $F \approx 2.8$ in form of

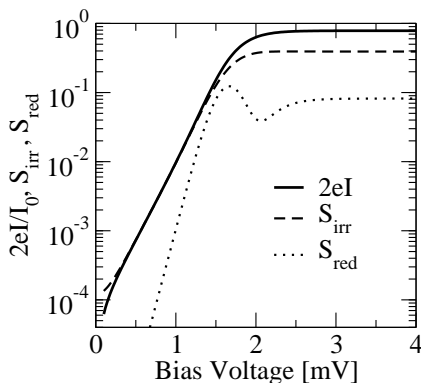


FIG. 3: Enlarged low bias region of Fig. 2. $2eI$, S_{red} and S_{irr} are plotted semi-logarithmically. The first part of the noise S_{irr} grows with bias as the current, providing a Poissonian noise contribution. The second part of the noise S_{red} becomes appreciable for $V > 2(\epsilon_{co} - \epsilon_{seq})/e$ and causes the total noise enhancement.

a plateau and do not recover a Poissonian value in the entire Coulomb blockade regime at all. In this case, S_{red} gives a large contribution that behaves with the same exponential behavior as the current rather than dropping faster than the current at low bias, as in Fig. 2). Thus the noise is enhanced in the entire Coulomb blockade regime. The term S_{irr} again provides the thermal noise at very low bias and a contribution of $2eI$ below the bias $V_b > (\epsilon_{seq} - \epsilon_{co})/e$. Above this bias, there is a redistribution between S_{irr} (losing) and S_{red} (winning), however, the sum of the two terms grows exactly like the current, leading to a constant (super-Poissonian) Fano factor.

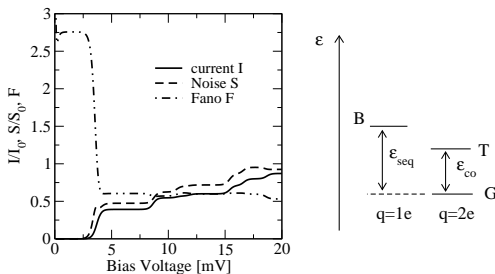


FIG. 4: *Left panel:* Current I and shot noise S vs. voltage for a double dot system with $k_B T = 0.05$, $t = 2$, $U = 12$, $U_{nn} = 4$ and $\epsilon = -6.3$. Super-Poissonian noise develops in the entire Coulomb blockade region. *Right panel:* the corresponding low energy spectrum, where $\epsilon_{co} < \epsilon_{seq}$.

Summarizing the above discussion we can distinguish three possible situations in the Coulomb blockade region: i) For $\epsilon_{co} > 2\epsilon_{seq}$ the sequential processes start at a bias before the excited states come into play, and the noise is Poissonian, i.e. $F = 1$ once the thermal noise becomes negligible. This is the case for Fig. 1, as sequential transport via the ground state G and the “bonding state” B takes place before the triplet state T can be reached from the bonding state B.

ii) For $\epsilon_{seq} < \epsilon_{co} < 2\epsilon_{seq}$ there is super-Poissonian noise $F > 1$ in the bias range $2(\epsilon_{co} - \epsilon_{seq})/e < V_b < 2\epsilon_{seq}/e$, see Fig. 2. This is due to the transport scenario discussed above, as for a bias in this range a thermally excited system can for a time do sequential transport through the excited states, before recovering to the ground state.

iii) For $\epsilon_{co} < \epsilon_{seq}$ we have $F > 1$ for the entire Coulomb blockade region. For a bias $2(\epsilon_{seq} - \epsilon_{co})/e < V_b < 2\epsilon_{seq}/e$ the situation is the same as in scenario ii). Below this bias range the physical picture due to Ref. 20 needs to be modified, as sequential transport is “blocked” (thermally activated) even out of the first excited state for $V_b < 2(\epsilon_{seq} - \epsilon_{co})/e$. Nevertheless, the Fano factor actually remains constant as the bias drops below $2(\epsilon_{seq} - \epsilon_{co})/e$, see Fig. 4.

However, as was pointed out in Ref. 14, the super-Poissonian noise behavior due to sequential tunneling processes in the Coulomb blockade regime is easily modified by co-tunneling processes. As elastic co-tunneling provides a Poissonian process are often much larger current (in the Coulomb blockade region) than the exponentially small sequential current, adding all contributions gives a Fano factor of nearly unity deep in the blockade region. Inelastic co-tunneling processes, on the other hand, can provide a “true” super-Poissonian noise around a bias ϵ_{co}/e above which the inelastic processes compete with the Poissonian elastic co-tunneling processes. Therefore, if co-tunneling processes dominate sequential processes (typically for ratios above $\Gamma/T \sim 10^{-314}$) there is either no super-Poissonian noise, if $\epsilon_{co} > 2\epsilon_{seq}$ as in scenario i), or, there is super-Poissonian noise starting around a bias of ϵ_{co}/e , similar to scenario ii). The experimental distinction of scenarios ii) and iii) can therefore be difficult: although the Fano factor looks different in pure sequential transport, if co-tunneling processes play a role, scenarios ii) and iii) will display qualitatively similar Fano factor behavior.

B. Asymmetric dot-electrode couplings

We now turn to the discussion of transport above the sequential tunneling threshold, i.e. in the bias region where electrons can tunnel sequentially through the DQD because they have sufficient energy to overcome the Coulomb blockade. For the symmetric situations as discussed above, the current and the noise increase monotonically in steps, where the step positions are determined by the many-body excitations of the DQD. For our DQD system, the noise in a symmetric transport situation remains sub-Poissonian (Fano factor $F < 1$) at all bias above the sequential tunneling threshold.

This is changed in situations with asymmetric couplings, e.g. when the coupling to the left electrode is suppressed relative to the coupling to the right electrode, $\Gamma_L/\Gamma_R < 1$. As all energy parameters are chosen to be the same as in the situation displayed in Fig. 1 the ground state is again a two electron state with $\epsilon_{co} > 2\epsilon_{seq}$. Hence

for the following discussion one should refer to the qualitative energy spectrum shown in the right panel of Fig. 1. In Fig.5 the upper graph depicts the Fano factor and the lower graph the absolute value of the current for various asymmetry ratios Γ_L/Γ_R (the current is negative for negative bias). In the symmetric case, represented by the solid line, the Fano factor as well as absolute current and the noise (that is not depicted here) show a fully symmetric behavior under the reverse of the bias voltage. The first plateau is reached when the transition from the doubly occupied ground state G ($q = 2e$) to the lowest single occupied state, the bonding state B, ($q = 1e$) becomes allowed at the sequential tunneling threshold ($V_b = 2\epsilon_{seq}/e$). At these plateaus the current, noise and Fano factor are functions of the coupling constants Γ_r only. At negative bias on the first plateau, the Fano factor is given by

$$F = \frac{4\Gamma_L^2 + \Gamma_R^2}{(2\Gamma_L + \Gamma_R)^2}. \quad (7)$$

This gives a value of $\frac{5}{9}$ at the first plateau for symmetric coupling. For positive bias voltage one needs to exchange Γ_L with Γ_R , respectively. This result can be related to previous work by some of us³³.

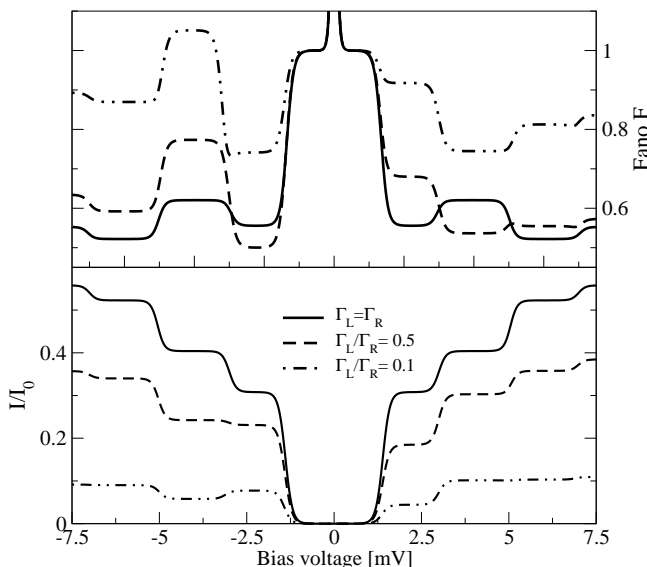


FIG. 5: Current I (absolute value) and Fano factor S vs. voltage for asymmetric coupling in a double dot system with $k_B T = 0.05$, $t = 2$, $U = 10$ and $U_{nn} = 5$, $\epsilon = -5.5$. For strong asymmetry negative differential conductance and super-Poissonian noise appear only for negative bias voltages. Note that due to the asymmetry the total line width $\Gamma = \Gamma_L + \Gamma_R$ and the current are reduced relative to the symmetric case.

For the curves with $\Gamma_L/\Gamma_R \neq 1$ there is a clear asymmetry in current and Fano factor. The first plateau value of the Fano factor is increased for positive bias and (for smaller asymmetry) decreased for negative bias according to the above expression for the Fano factor. Further

suppression of the left coupling leads to a region of negative differential conductance (NDC) and eventually a super-Poissonian Fano factor on the second plateau at negative bias (see dash-dotted curve for $\Gamma_L/\Gamma_R = 0.1$). The reason for the current suppression and asymmetric behavior is the interplay of the asymmetric couplings and the internal electronic structure. The occupation of the states participating in transport at the plateaus is highly sensitive to the asymmetric couplings.

Let us consider the first plateaus (positive and negative bias) of the current in the case $\Gamma_L/\Gamma_R = 0.1$. For negative bias, in contrast to the symmetric case where the ground state G and the bonding state B are equally occupied, we have now a higher probability to be in the state G than in the state B. This is due to the fact that it is “easy” to populate the DQD from the right but “difficult” to depopulate the DQD in direction of the left electrode because of the suppressed coupling. As a consequence the system is occupied by two electrons most of the time. The reverse holds for positive bias, where the dot is most often occupied by one electron and consequently the probability to be in the state B on the first plateau is higher than to be in the ground state G.

To obtain the current I we need to consider the relevant current rates W^I in addition to the probabilities of the various states. On the first plateaus, the relevant current rates $W_{G \rightarrow B_\sigma}^I$ from ground state to bonding state(s) (with given spin σ) at negative bias are equal in magnitude to the reverse rates $W_{B_\sigma \rightarrow G}^I$ at positive bias (independent of the spin σ of B_σ). Solving the master equation, as a result of the coupling asymmetry the probability p_G to be in state G on the first plateau at negative bias is however larger (almost twice) than the occupation p_{B_σ} for states B_σ on the first plateau at positive bias. The combination of the same relevant current rate but different occupations leads to a higher (absolute) value of the current on the first plateau at negative bias than on the corresponding plateau at positive bias. To be concrete, if we consider the currents on the left interface of the DQD we have at negative bias a current with absolute value $|2W_{G \rightarrow B}^I p_G|$ which is almost twice as large (for $\Gamma_L/\Gamma_R = 0.1$) than the current $W_{B \rightarrow G}^I 2p_{B_\sigma}$ going through the left interface at positive bias. Here, the factors of two originate from the spin summation over the bonding state doublet.

On the first plateau the Fano factor is monotonically increasing for positive bias with decreasing Γ_L/Γ_R until it would reach the Poissonian value $F \rightarrow 1$ for very large asymmetry, resembling the noise of an effective single barrier. For negative bias on the first plateau, the Fano factor (given by Eq. 7) is not monotonic: it first decreases until it reaches $F = 1/2$ for $\Gamma_L/\Gamma_R = 0.5$, then it increases until it also would reach the Poissonian value for large asymmetry. This non-monotonic behavior reflects the interplay of asymmetry and different spin multiplicity of the relevant states G and B.

At the second plateau the transition from the bonding state B to the first excited triplet state T ($q = 2$) becomes

possible and thus provides a second current channel. The stationary probabilities are redistributed in the following way: For negative bias, the states G and each of the three triplet states T_m , $m \in -1, 0, 1$ have approximately equal occupation (within 10 percent). As a consequence of the threefold spin multiplicity of the triplet the probability of the ground state decreases to less than one third of its value on the first plateau. The bonding state B also loses some of its (already small) probability to the competing triplet states. The tunneling processes from the triplet state(s) T to the bonding state(s) B contribute an additional current via the current rates $W_{T \rightarrow B}^I$ (per triplet state and spin of B). However, even when summing over all the triplet contributions the resulting current is too small to compensate the loss from the processes involving the ground state. Therefore a region of negative differential conductance (NDC) appears as soon as the triplet states play a role in transport for negative bias (at the considered coupling asymmetry). The NDC is accompanied by a (relatively) enhanced noise because the competing processes involving the ground state and the triplets have sufficiently unequal rates $W_{G \rightarrow B}^I$ and $W_{T \rightarrow B}^I$ to form 'slow' and 'fast' transport channels. This competition leads to the super-Poissonian Fano factor as depicted in Fig. 5.

For positive bias on the second plateau the situation is quite different. Here, the DQD remains mostly in the bonding state B, i.e. there is no major loss of occupation for the bonding state (about 10 percent). Again the current leaving the dot consists of two additive con-

tributions. In addition to the ground state contribution already present on the first plateau, the transitions between bonding to the triplet states add a large contribution and thus the current increases stepwise to a second, higher plateau.

The above illustrates that although for one bias direction (here positive) the current and shot noise show generic behavior (and the Fano factor is always sub-Poissonian), the situation can be quite different for the reverse bias. As such asymmetries are easily verified in an experiment, we can learn much about the underlying asymmetries of the couplings and the spin multiplicities of the states participating in transport. Note that the NDC and super-Poissonian noise would completely disappear if we would take the onsite Coulomb repulsion $U \rightarrow \infty$. Due to a finite U the singlet ground state can benefit from 'local singlets', i.e. states with two electrons of opposite spin on the same dot, whereas there is no equivalent for triplet states. Therefore, the singlet ground state has a lower energy and different transition rates as compared to the triplet states, both of which are necessary conditions for the NDC and super-Poissonian noise in the considered single-level model.

C. Detuned level energies

The discussion above serves as a basis to qualitatively understand transport in the more complicated situation when the symmetry of the DQD Hamiltonian itself is broken, rather than merely its coupling to the electrodes. In the following, we detune the level energies $\epsilon_1 - \epsilon_2 = \epsilon_{12}$ and also vary the inter-dot hopping t while the other parameters of the dot system remain the same and the couplings remain symmetric, $\Gamma_L = \Gamma_R$. For an experiment, this implies a gate electrode for each dot that can be controlled separately. Similar to above in Fig. 5, if roughly $|\epsilon_1 - \epsilon_2| = |\epsilon_{12}| > |t|$, NDC and super-Poissonian noise can be realized at some bias.

In Fig. 6 we show current and Fano factor for different level detuning ϵ_{12} . The black solid line corresponds to symmetric couplings and resonant levels $\epsilon_1 = \epsilon_2$. It is the same as depicted in Fig.5. If we start detuning the levels, i.e. $\epsilon_{12} \neq 0$ we change our excitation energies and the states become more localized on the dot with lower energy (here the right dot). Consequently, we find the current and Fano factor plateaus at different (energy) positions as before, with different length of the plateaus. Note that the current on the first plateau only weakly changed for all ϵ_{12} considered here. This is due to the fact that despite of the changed Hamiltonian, the tunneling rates from ground state to bonding state as well as the occupations of these states are almost the same. The occupations on the first plateau are also only weakly dependent on the sign of the bias, quite different to the situation with asymmetric couplings considered above. Only with an even stronger level detuning would the current be significantly changed on the first plateau.

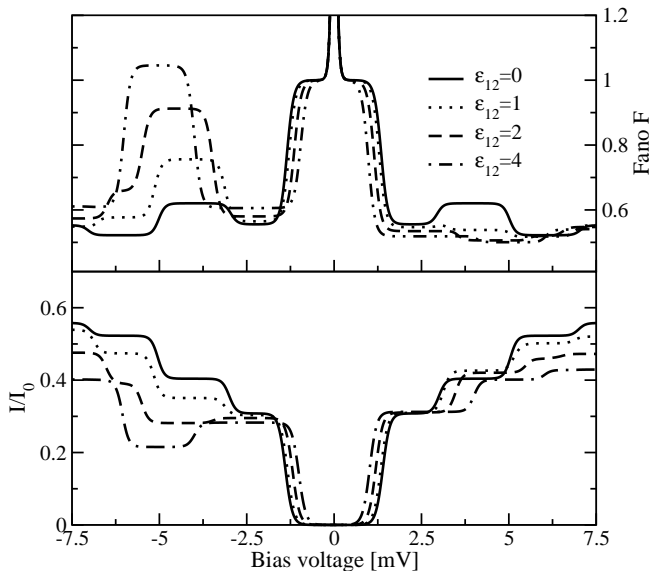


FIG. 6: Current I (absolute value) and Fano factor S vs. voltage for various values of level detuning ϵ_{12} but with symmetric couplings to the leads and other energy parameters equal to the situation depicted in Fig.1. Stronger detuning ϵ_{12} leads to NDC and eventually super-Poissonian noise. In contrast to Fig.5, the bias (energy) positions of current and noise features are changed due to the modified dot Hamiltonian.

However, the considered detuning of levels still leads to NDC and eventually to a super-Poissonian Fano factor, e.g. for $\epsilon_{12} = 4$) at negative bias. The effect of triplet states on the second plateau is qualitatively the same as in the scenario with asymmetric coupling discussed above. For positive bias the current remains monotonic and the Fano factor sub-Poissonian. In agreement with previous results⁸ the maximum current at very large bias (not shown) decreases with increased detuning although the total coupling Γ remains unchanged.

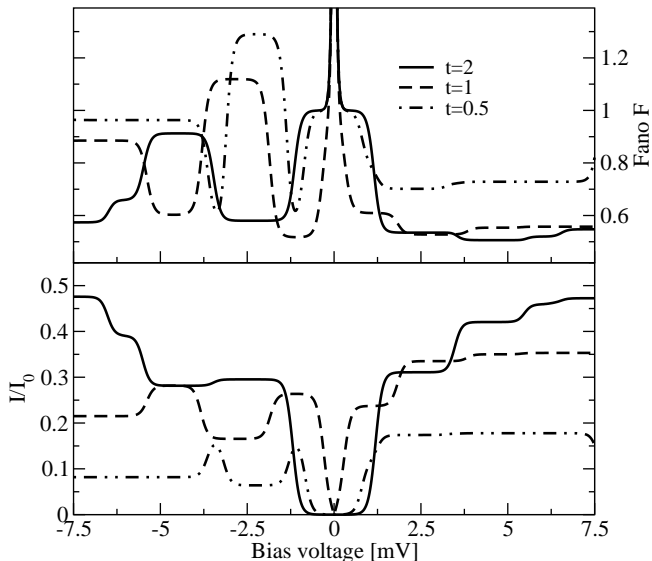


FIG. 7: Current I (absolute value) and Fano factor S vs. voltage for various “hopping” parameters t and a level detuning of $\epsilon_{12} = 0.2$, symmetric coupling to the leads and otherwise same parameters as in the situation depicted in Fig. 1. Reduced hopping causes a smaller total current although super-Poissonian noise and NDC develop similarly as in Fig.6.

Instead of further increasing the level detuning one can also achieve “localization” of states by decreasing the inter-dot hopping t . Let us consider again the symmetrically coupled system ($\Gamma_L = \Gamma_R$) at a fixed detuning of $\epsilon_{12} = 2$ for various values of the inter-dot hopping t (see Fig.7). The solid line corresponds again to the case, in which $\epsilon_{12} = 2$ and $t = 2$, as was also depicted in Fig.6(dashed line). As expected, the plateaus of the current are again asymmetric since we have detuned level energies. If we now decrease t , the bonding state and the ground state will be separated by only a very small energy (as $U_{nn} = 5$ and $(\epsilon_1 + \epsilon_2)/2 = 5.5$) and thus the Coulomb blockade almost disappears. For positive bias both current and Fano factor (noise) behave generically. The first plateau for negative bias is again due to tunneling processes involving the states B and G. At the second plateau the triplet T starts participating in the transport and is strongly occupied, resulting in NDC and super-Poissonian noise as discussed above. At even more negative bias there exists a second region of NDC (for the cases $t = 1$ and $t = 0.5$). This is where the

anti-bonding state (not depicted in the spectrum in the right panel of Fig. 1) is also contributing to the transport. The maximum current at large bias (not shown) depends on the inter-dot hopping t ⁸ if the dot levels are out of resonance.

From Fig. 6 and Fig. 7 one can conclude that a higher degree of localization of the states participating in transport, achieved either by a strong detuning of level energies or a decrease in the inter-dot hopping, favors transport features such as NDC and makes the current more and more noisy, leading eventually to super-Poissonian noise. Reducing the hopping (at fixed detuning) therefore has a similar effect on transport as a larger detuning at fixed hopping. However, as the DQD spectrum differs non-linearly between different parameter sets with identical ratio ϵ_{12}/t the resulting transport curves can not be scaled, but depend explicitly on the value of each parameter.

D. Comparison with related theoretical work

For reference we show in Fig. 8 the current and Fano factor for a fully symmetric system, i.e. equal couplings to left and right and resonant level energies but for different values of the inter-dot hopping t . As expected all curves behave symmetric under the reverse of bias. Similar to Fig. 7, for smaller hopping t the sequential tunneling threshold, determined by the energy distance of the states G and B, becomes very small for the chosen parameters and thus the Coulomb blockade almost disappears. Since there is no asymmetry in the system, not in the couplings, nor in the energy levels, we do not expect and do not find regions of NDC and/or super-Poissonian noise. This is specific to this DQD system, in which there are only interfacial dots and thus there is always a finite probability for the electrons to depopulate the dot structure. In contrast, in chains of three and more quantum dots we do find super-Poissonian noise even for a fully symmetric system¹⁸, if the ratio U_{nn}/t is sufficiently large. In these more complex systems the enhancement of the noise is due to a combination of the non-local many-body wave functions and the states with higher total spin ($3/2$).

Note that although the current (Fano factor) does very much depend on the value of the hopping t for the low bias regime depicted in Fig. 8, the maximum current at very large bias (not shown) is actually independent of the hopping t . This is due to our neglect of off-diagonal matrix elements of the reduced density matrix. Such off-diagonal elements have been included in the work of Ref. 8 by Ellatari and Gurvitz. They have studied the shot noise through two coupled quantum dots via a quantum rate equation, i.e. a master equation involving also the off-diagonal elements of the reduced density matrix. The effect of off-diagonal elements on transport are negligible for the weak coupling situation we consider, but become increasingly important, if the coupling Γ becomes

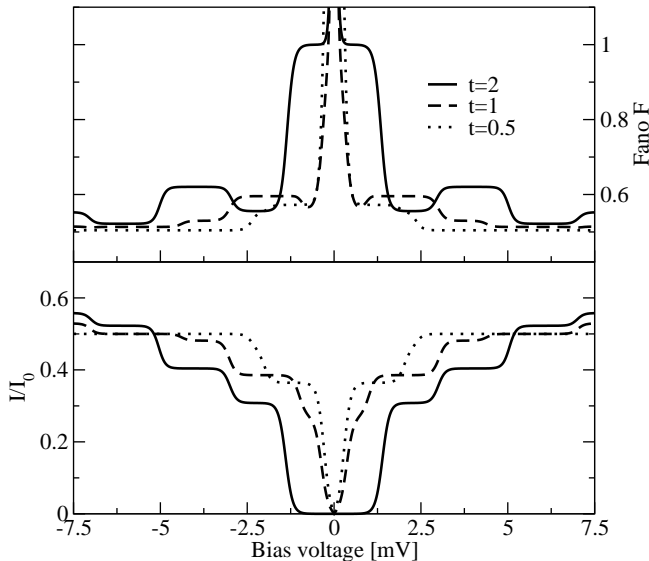


FIG. 8: Current I (absolute value) and Fano factor S vs. voltage for different values of “hopping” t without level detuning ($\epsilon_{12} = 0$) for symmetric couplings and same parameters as in the situation depicted in Fig. 1. Note that current and Fano factor are both symmetric under the reverse of bias voltage, since there is no source of asymmetry.

comparable to the intrinsic energy scales of the dot system, such as the hopping energy t . Naturally, a straight perturbative approach as ours does not make sense for such large Γ (at least not to first order in Γ), so our results apply to the explicit case of weak coupling, such that Γ is the smallest energy scale. The approach of Ref. 8, introduced in detail in Ref. 34, is not explicitly restricted to a small Γ . Under certain assumptions and restrictions the contributions from all the lead states can be “integrated out” and a quantum rate equation (still linear in Γ) for the relevant parts of the reduced density matrix is obtained. After solving the quantum rate equation, the current and the shot noise can be computed.

However, it is important to note that the approach of Ref. 8,34 imposes severe restrictions on the transport situations it can treat. The applied bias has to be very large, such that all states (or excitations) of the dots that are considered for transport lie well in between the Fermi levels (chemical potentials) of the electrodes. On the other hand, the states not considered for transport should be very far away from the chemical potentials of the leads. Figuratively speaking, the approach of Ref. 8 applies to the center of a very long (in principle, infinitely long) plateau of the I-V characteristics. Such plateaus are not realized for the situations we considered, with the exception of the last plateau, when the bias is much larger than *all* excitations (or energies) of the dot system. In Ref. 8 the large bias regime for a spinless version of our Hamiltonian (implying also $U = \infty$) and the cases $U_{nn} = 0$ as well as $U_{nn} = \infty$ were considered. For $U_{nn} =$

0 we have a non-interacting system of spinless fermions, whereas for $U_{nn} = \infty$ only states with at most a single (spinless) electron on the dot system are relevant. The results of Ref. 8 for current and shot noise for $\Gamma/t \ll 1$ approach our results (not shown), as it should be. If Γ/t is not negligibly small, corrections to our results become noticeable that reduce the current and the shot noise, but also the Fano factor. If $\Gamma \gg t$ the system turns into an effective single barrier system, so that the current is $\propto t^2/\Gamma$ and the noise becomes Poissonian, $F \rightarrow 1$.

Recently, two groups^{11,12} claimed to have extended the approach of Ref. 8 to the arbitrary bias regime. The results of Ref. 12 for the current on single dot systems are in perfect agreement with earlier work by us¹³. This is expected, as there are no possible “coherence effects” in a single level system, if spin is conserved in tunneling. Whereas Ref. 12 does not discuss interacting double dot systems (or shot noise) Ref. 11 also considers the spinless version of our DQD Hamiltonian. They discuss both current and shot noise through a double dot system with resonant levels ϵ and an infinitely large intra-dot repulsion U , starting from an empty dot system as a ground state. Therefore, they can only consider two possible regimes with finite current. i) For a bias $2\epsilon < eV_b < 2(\epsilon + U_{nn})$, they consider to have at most one electron on the double dot system. In this case they recover the result of Ref. 8 for the case $U_{nn} = \infty$. ii) For bias larger than all excitation energies ($eV_b > 2(\epsilon + U_{nn})$) they recover the *non-interacting* result of Ref. 8. In contrast, in our approach there are two additional possible transport situations that arise from the fact that there are two eigenstates in a singly occupied double dot system, namely the bonding (B) and the anti-bonding (A) state that differ by the energy $2t$. Therefore, in general there will be two steps corresponding to excitations of the bonding state ($\epsilon - t$) and the anti-bonding state ($\epsilon + t$) out of the ground state ($\epsilon = 0$) and another two steps corresponding to the excitation energies to the doubly occupied state at $\epsilon + U_{nn} - t$ and $\epsilon + U_{nn} + t$. Hence, the current and noise characteristics for the double dot system with $U \rightarrow \infty$ should show four steps, unless broadening effects due to temperature or the line width Γ are so large that they smear out the steps. In Ref. 11, Fig. 6, there are only two steps which are broadened by temperature only (via the Fermi functions). Therefore, at best it corresponds to a situation for which $t < \Gamma \ll k_B T$, i.e. a situation in which the system resembles more an effective single barrier system at high temperature.

The “concatenation” of two results by Ref. 11 that are derived under the assumption of effectively infinite bias in Ref. 8 also leads to the peculiar effect that the current exhibits NDC behavior for a ratio of $\Gamma/t > 2$. While it is possible that a fully spatially symmetric system can display NDC¹⁸, in our weak coupling theory ($\Gamma \ll t$) of the DQD system NDC can only occur with broken symmetry such as detuned level energies, asymmetric couplings etc. as discussed in this paper.³⁵ The NDC effect in Ref. 11 occurs in a parameter regime

where our theory clearly does not apply. It would be interesting to see whether other approaches like the ones based on equation of motion methods^{27,36} can confirm or disprove the NDC effect displayed in Fig. 6 of Ref. 11. Very recent work of Ref. 37 includes level renormalization terms left out by Ref. 8,11 that modify the current characteristics qualitatively in the regime $\Gamma \gg t$. This shows that the inclusion of off-diagonal elements of the density matrix is a rather delicate matter.

IV. SUMMARY

In summary we have discussed transport through a double quantum dot (DQD) system with both intra- and inter-dot Coulomb interactions in the sequential transport picture, as currently studied by several experimental groups. We found that the behavior of the shot noise in the Coulomb blockade is directly related to the underlying low energy spectrum of the DQD system characterized by two intrinsic energy scales, the sequential tunneling energy ϵ_{seq} and the first vertical excitation energy out of the ground state, ϵ_{co} . For a symmetric system in the Coulomb blockade we distinguished between three scenarios: i) For a first vertical excitation energy that is smaller than twice the sequential tunneling energy $\epsilon_{co} > 2\epsilon_{seq}$ the Fano factor (noise) is always sub-Poissonian, i.e. $F < 1$, as sequential processes start before excited states come into play. ii) If $\epsilon_{seq} < \epsilon_{co} < 2\epsilon_{seq}$ thermally activated sequential transport leads to super-Poissonian Fano factors in the bias range $2(\epsilon_{co} - \epsilon_{seq})/e < V < 2\epsilon_{seq}/e$. iii) For the case $\epsilon_{co} < \epsilon_{seq}$ the Fano factor remains super-Poissonian in the entire Coulomb blockade regime. Our findings are valid for arbitrary ground state charges and also apply to larger systems with more than two coupled dots, as they depend only on the above mentioned generic energy

scales of the interacting dot system.

Additionally, we discussed the effect of asymmetries in the system realized by either asymmetric couplings to the electrodes or by detuning the quantum dot levels out of resonance with each other. In the case of asymmetric dot-electrode couplings we obtained an asymmetric current voltage characteristics as has been observed in experiments before. For very strong asymmetry negative differential conductance and eventually super-Poissonian noise with Fano factors $F > 1$ develop. These features develop at the same energy positions, i.e. at the same bias voltage for any asymmetry ratio Γ_L/Γ_R since the DQD spectrum remains unchanged. In contrast detuning the dot levels out of resonance also leads to NDC and super-Poissonian noise for sufficiently strong asymmetry, but now at voltages that depend on the strength of the asymmetry as the DQD spectrum is changed. These features only appear for one bias direction, $V < 0$ or $V > 0$, depending on which coupling Γ_r (r =right,left) is suppressed or which quantum dot has a lower level energy. Furthermore, we found that at a fixed detuning ϵ_{12} the current is reduced with decreasing inter-dot hopping t . The latter results in a stronger localization of states on individual dots similar to the case of strongly detuned quantum dots. Therefore a weaker inter-dot hopping and a stronger detuning at fixed inter-dot hopping cause similar transport characteristics.

To conclude, we have shown that transport properties of double quantum dots, in particular the shot noise, show a strong sensitivity on the internal electronic structure and the coupling strengths to the electrodes. This sensitivity should allow for a detailed characterization of these energy scales in a given experiment.

Acknowledgments. We acknowledge helpful discussions with Maarten Wegewijs, Bernhard Wunsch, Jonas Pedersen and Andreas Wacker, and the financial support by the DFG via the Center for Functional Nanostructures (CFN).

¹ 'Mesoscopic Electron Transport', eds. L. L. Sohn, L. P. Kouwenhoven, and G. Schön, NATO ASI Series Vol. 345, (Kluwer Academic Publishers, 1997).

² W.G. van der Wiel, S. de Franceschi, J. M. Elzerman, T. Fujisawa, S. Tarucha, and L. P. Kouwenhoven, Rev. Mod. Phys. **75**, 1 (2003).

³ S. S. Safonov, A. K. Savchenko, D. A. Bagrets, O. N. Jouravlev, Y. V. Nazarov, E. H. Linfield, and D. A. Ritchie, Phys. Rev. Lett. **91**, 136801 (2003).

⁴ A. Nauen, F. Hohls, N. Maire, K. Pierz and R. J. Haug, Phys. Rev. B **70**, 033305 (2004).

⁵ S. W. Jung, T. Fujisawa, Y. Hirayama and Y.H. Jeong, Appl. Phys. Lett. **85**, 768 (2004).

⁶ G.-E. Onac, Dissertation, TU Delft (2005).

⁷ G. Michalek and B. R. Bulka, Eur. Phys. J. B **28**, 121 (2002).

⁸ B. Elattari and S. A. Gurvitz, Phys. Lett. A **292**, 289 (2002).

⁹ G. Kiesslich, A. Wacker, E. Schoell, A. Nauen, F. Hohls, and R. J. Haug, phys. stat. sol. (c) **0**, 1293 (2003); G. Kiesslich, A. Wacker, and E. Schoell, Phys. Rev. B **68**, 125320 (2003).

¹⁰ A. Cottet and W. Belzig, Europhys. Lett. **66**, 405 (2004).

¹¹ I. Djuric, B. Dong, and H. L. Cui, cond-mat/0406679.

¹² X. Li, J. Luo, Y. Yang, P.Cui, and Y. Yan cond-mat/0409643

¹³ A. Thielmann, M. H. Hettler, J. König, and G. Schön, Phys. Rev. B **68**, 115105 (2003); *ibid.* Phys. Rev. B **71**, 045341 (2005).

¹⁴ A. Thielmann, M. H. Hettler, J. König, and G. Schön, Phys. Rev. Lett. **95**, 146806 (2005)

¹⁵ A. N. Jordan and E. V. Sukhorukov, Phys. Rev. Lett. **93**, 260604 (2004).

¹⁶ J. Koch and F. von Oppen, Phys. Rev. Lett. **94**, 206804 (2005).

¹⁷ C. Flindt, T. Novotny, and A.-P. Jauho, AIP Conf. Proc.

- 780**, 442 (2005).
- ¹⁸ J. Aghassi, A. Thielmann, M.H. Hettler, and G. Schön, cond-mat/0505345.
 - ¹⁹ Ya. M. Blanter and M. Büttiker, Phys. Rep. **336**, 1 (2000).
 - ²⁰ W. Belzig, Phys. Rev. B **71**, 161301(R) (2005).
 - ²¹ A. K. Huettel, S. Ludwig, K. Eberl, J. P. Kotthaus, Phys. Rev. B **72**, 081310(R) (2005).
 - ²² M. Sigrist, T. Ihn, K. Ensslin, D. Loss, M. Reinwald, and W. Wegscheider, cond-mat/0508757
 - ²³ T. Hatano, M. Stopa, T. Yamaguchi, T. Ota, K. Yamada, and S. Tarucha, Phys. Rev. Lett. **93**, 066806 (2004)
 - ²⁴ L. DiCarlo, H.J. Lynch, L.I. Childress, K. Crockett, C.M. Marcus, M.P. Hanson, A.C. Gossard, Phys. Rev. Lett. **92**, 226801 (2004)
 - ²⁵ J.R. Petta, A. C. Johnson, J. M. Taylor, E.A. Laird, A. Yacoby, M.D. Lukin, C.M. Marcus, M.P. Hanson, A.C. Gossard, Science **309**, 2180, (2005).
 - ²⁶ M. H. Hettler, W. Wenzel, M. R. Wegewijs, and H. Schoeller, Phys. Rev. Lett. **90**, 076805 (2003).
 - ²⁷ B. R. Bulka and T. Kostyrko, Phys. Rev. B **70**, 205333 (2004).
 - ²⁸ J. König, H. Schoeller, and G. Schön, Phys. Rev. Lett. **76**, 1715 (1996); J. König, J. Schmid, H. Schoeller, and G. Schön, Phys. Rev. B **54**, 16820 (1996).
 - ²⁹ S. Hershfield, J. H. Davies, P. Hyldgaard, C. J. Stanton, and J. W. Wilkins, Phys. Rev. B **47**, 1967 (1993).
 - ³⁰ A. N. Korotkov, Phys. Rev. B **49**, 10381 (1993).
 - ³¹ The magnetic quantum number, i.e. the z-component of the total spin plays no role in our spin degenerate DQD system without magnetic fields and normal metal electrodes.
 - ³² E. V. Sukhorukov, G. Burkard, and D. Loss, Phys. Rev. B **63**, 125315 (2001).
 - ³³ Our first plateau value corresponds to the second plateau of Ref. 13 (which considered spin non-degenerate levels), with the further requirement that Γ_L and Γ_R need to be exchanged as the plateau is reached by a transition from a higher charge state to a lower charge state.
 - ³⁴ S. A. Gurvitz, Phys. Rev. B **57**, 6602 (1998).
 - ³⁵ NDC can be achieved in local multi-level systems, provided that one level couples sufficiently weaker than the other(s). However, the considered non-local two dot system can not be mapped to such a system without breaking the spatial symmetry.
 - ³⁶ J. N. Pedersen and A. Wacker, Phys. Rev. B **72**, 195330 (2005).
 - ³⁷ B. Wunsch, M. Braun, J. König and D. Pfannkuche, Phys. Rev. B **72**, 205319 (2005).